β-Pareto Set Prediction for Bi-Objective Reliability-Based Design Optimization

Dong-Shin Lin
Graduate Student
e-mail: linds@solab.me.ncku.edu.tw

Chun-Min Ho
Research Assistant
e-mail: hocm@solab.me.ncku.edu.tw

Kuei-Yuan Chan[1]
Associate Professor of Mechanical Engineering
e-mail: chanky@mail.ncku.edu.tw

National Cheng Kung University
Tainan, 70101, Taiwan

In this research, we investigate design optimization under uncertainties for problems with two objectives. Reliability-based design optimization (RBDO) that considers uncertainties as random variables and/or parameters and formulates constraints probabilistically has received extensive attention. However, research to date has focused primarily on single-objective problems only. We extend RBDO to problems for which multiple objectives are optimized simultaneously. Each constraint reliability value results in a Pareto set. The set of all Pareto frontiers at the various reliability values is denoted as the β-Pareto set. We study the relations between the deterministic Pareto set and the β-Pareto set and then develop a method to systematically determine the exact β-Pareto set of bi-objective linear programming problems. The method is also extended to predict the β-Pareto set of nonlinear problems using the sandwich technique. As a result, we are able to accurately predict the β-Pareto set in the objective space without solving multiple multi-objective optimization problems at various reliability levels. In the early stage of the product design process, the proposed approach can help decision-makers efficiently to determine how product performance varies with reliability level. [DOI: 10.1115/1.4004442]

Keywords: bi-objective optimization, design under uncertainty, reliability-based design optimization, Pareto frontiers, decision-making process

1 Introduction and Literature Review

Design is a multi-objective decision-making process that considers manufacturing, cost, aesthetics, usability, and many other product attributes. Decisions often have to be made under various operating and environmental uncertainties. Reliability-based design optimization (RBDO) allows designers to obtain optimal product specifications when the desired target reliability is known. If the target reliability is unknown, the decision-making process becomes challenging. For example, the reliability of a vehicle structure generally compromises other vehicle performances. Design engineers generally have no basis for judging how the trade-off between objectives changes with reliability. Arbitrarily selecting a reliability value might result in a design that is either too conservative or too risky. Selecting a very high reliability value will also limit design options. A systematic approach is needed to assist decision-making under uncertainty when quick estimates of design outcomes are required.

This research investigates solutions to bi-objective optimization problems under uncertainties quantified as random design variables and/or random parameters. Equation (1) shows the generalized mathematical formulation with objectives $\mathbf{f}=\{f_1, f_2\}$ that are functions of the means of random variables only. The constraints in Eq. (1) are formulated probabilistically with failure probabilities being less than or equal to P_f. Constraint reliabilities are therefore $(1-P_f)$. All uncertainties $\mathbf{X}$ are assumed to be Gaussian with means $\boldsymbol{\mu}_\mathbf{X}$ as design variables and standard deviations (STDs) $\boldsymbol{\sigma}_\mathbf{X}$ as fixed constants. In this problem setup, we consider deterministic variables $\mathbf{x}$ as a special case with zero variance. Deterministic constraints that are not functions of random variables are considered as a special case with P_f being zero. All $\mathbf{X}$ are uncorrelated with each other and all equality constraints are implicitly removed with $\mathcal{K}$ being the constraint set

$$\begin{aligned} &\min_{\boldsymbol{\mu}_\mathbf{X}} \mathbf{f}(\boldsymbol{\mu}_\mathbf{X}) \\ &\text{s.t. } \Pr[g_j(\mathbf{X})>0] \le P_f, \forall j \in \mathcal{K} \\ &\mathbf{X} \sim N(\boldsymbol{\mu}_\mathbf{X}, \boldsymbol{\sigma}_\mathbf{X}^2) \end{aligned} \tag{1}$$

Values of the failure probability P_f in Eq. (1) directly affect the feasible space of Eq. (1) and consequently change the optimal solutions. Let $\mathcal{F}$ be the deterministic feasible space of constraints $\mathbf{g} \le 0$. The mapping of $\mathcal{F}$ to the objective space forms the attainable set $\mathcal{A}$.

Definition 1.1. *Consider two design points $\mathbf{x}_i$, $\mathbf{x}_j$ in $\mathcal{F}$. We say that $\mathbf{x}_i$ dominates $\mathbf{x}_j$ if and only if*

$$f_k(\mathbf{x}_i) < f_k(\mathbf{x}_j) \forall k \tag{2}$$

If the set of all $\mathbf{x}_i$ in $\mathcal{F}$ satisfying Eq. (2) is null, we say that $\mathbf{x}_j$ is a nondominated design. Let the mappings of $\mathbf{x}_i$ and $\mathbf{x}_j$ to the objective space be $\mathbf{f}_i$ and $\mathbf{f}_j$, respectively. The subset of $\mathcal{A}$ with all nondominated solutions forms the Pareto set, denoted as $\mathcal{P}$. $\mathbf{f}^*$ represents points on the Pareto set.

Definition 1.2. *A probabilistic feasible space $\mathcal{F}_p(P_f)$, defined in Eq. (3), is the space of all $\boldsymbol{\mu}_\mathbf{X}$ satisfying the probabilistic constrains in Eq. (1).*

$$\begin{aligned} \mathcal{F}_p(P_f) = \{&\boldsymbol{\mu}_\mathbf{X} \in \mathbb{R}^n : \Pr[g_j(\mathbf{X})>0] \le P_f \ \forall j \in \mathcal{K}, \\ &\mathbf{X} \sim N(\boldsymbol{\mu}_\mathbf{X}, \boldsymbol{\sigma}_\mathbf{X}^2)\} \end{aligned} \tag{3}$$

Definition 1.3. *A β-Pareto set $\mathcal{P}_\beta$ is the set of all Pareto frontiers at different P_f values.*

Numerous studies related to the β-Pareto set have been published. Li et al. used a multi-objective framework to study the relations between manufacturing cost and dimensional variations in multistation assembly processes [1] and the effects of

[1]Corresponding author.

Manuscript received July 7, 2010; final manuscript received May 19, 2011; published online July 27, 2011. Assoc. Editor: Wei Chen.

 Copyright © 2011 by ASME

Downloaded 27 Jul 2011 to 140.116.71.27. Redistribution subject to ASME license or copyright; see http://www.asme.org/terms/Terms_Use.cfm

manufacturing variations in a fuel injector on engine emissions [2]. Results of β-Pareto sets at different uncertainty levels (dimensional tolerance and manufacturing variations, respectively) were presented. Levi et al. generated a β-Pareto set of a cantilever beam with respect to buckling under material uncertainties [3]. In Ref. [4], Singh and Minsker investigated the simultaneous effects of uncertainty on the cost and residual values of various groundwater remediation designs.

Similar studies have been conducted on stochastic multi-objective programming (SMP) problems; for example, see Refs. [5–7]. Rommelfanger used both random and fuzzy concepts to model uncertainties in SMP by converting multiple objectives into a single objective problem using a weighted sum [8]. Tonon et al. considered SMP with both random and fuzzy uncertainties in tunnel design [9]. In their work, probabilistic constraints are converted into equivalent deterministic ones, allowing standard deterministic optimization techniques to be applied. Only parameter uncertainties are considered in SMP and the solution approaches are mainly focused on constructing the Pareto set with known uncertainties at a specified reliability level.

Figure 1 shows how the β-Pareto set is generated in the present study. After a P_f value is determined, the Pareto set $\mathcal{P}$ with respect to P_f is generated. Standard approaches for generating a Pareto set involve finding a finite number of nondominant design points via a weighted sum [10] or a constraint method [11] and then connecting these nondominant points to approximate the true Pareto set. The number of nondominant design points required is restricted primarily by the computational cost since each nondominant design point requires a full optimization run of the equivalent problem. If the Pareto set of a given P_f is obtained, one has to repeat the entire process to generate another Pareto set for a different P_f.

The process in Fig. 1 is computationally intensive and cannot be used to predict a Pareto set at an untested P_f value. If none of the existing β-Pareto sets are satisfactory to a designer, the process is repeated at a different P_f value. This removes the main benefits of having a Pareto set, which are that all solutions in the set are optimal and that decision-makers can select the best design based on their preferences or other design considerations. Imagine that the Pareto sets of a problem with $P_f = 0.1, 0.2, 0.3$ are provided to a decision-maker. The decision-maker might be willing to trade-off reliability with the objectives in Eq. (1); for example, improve P_f to 0.05 or better. Several new Pareto sets have to be computed before decisions can be made. Alternatively, the Pareto sets at these P_f values can be established based on the deterministic Pareto set.

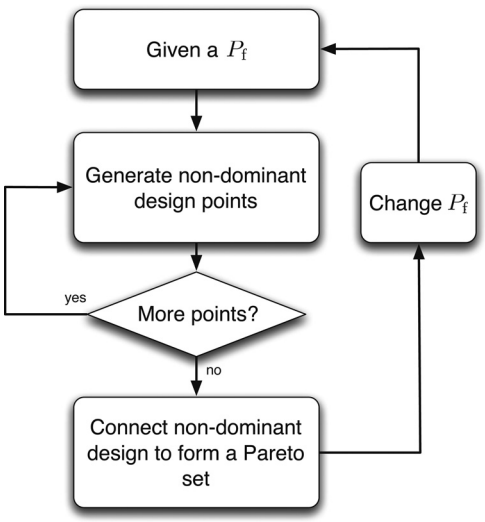

Fig. 1 Existing approach for generating β-Pareto set

In this research, we develop a systematic approach for identifying the β-Pareto set for bi-objective optimization problems under random uncertainties. The rest of this paper is organized as follows. An exact method for predicting the β-Pareto set of linear systems is proposed in Sec. 2. This method is extended to handle nonlinear problems in Sec. 3. A vehicle design problem is studied using the proposed method in Sec. 4. Conclusions are provided in Sec. 5.

2 Proposed Method for β-Pareto Generation With Linear Problems

In this section, we study the solutions to the bi-objective linear programming (BOLP) under uncertainty shown in Eq. (4). All functions, including objectives and constraints, are linear. Design variables are the means of all uncertainties. Figure 2 shows a flowchart of the proposed method for generating the β-Pareto set for BOLP under uncertainty. The deterministic Pareto set is first generated using the method proposed by Dauer and Liu [12]. This approach searches for nondominant extreme points in the objective space by constructing frame vectors of the reduced cost coefficient matrix $\mathbf{R}$ based on the solution of the extreme points

$$\begin{aligned} &\min_{\boldsymbol{\mu}_x} \mathbf{f} = \mathbf{C}^T \boldsymbol{\mu}_x \\ &\text{subject to } \Pr[\mathbf{g} = \mathbf{A}^T \mathbf{X} - \mathbf{b} > \mathbf{0}] \le P_f \\ &\mathbf{X} \sim (\boldsymbol{\mu}_x, \boldsymbol{\sigma}_x^2) \end{aligned} \tag{4}$$

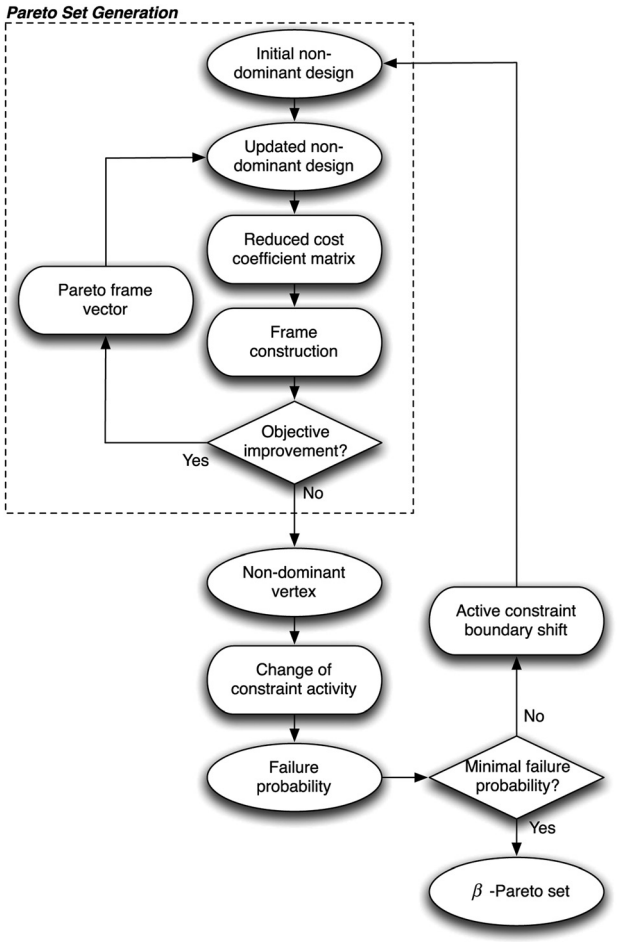

Fig. 2 Constructing the β-Pareto set of a BOLP under uncertainty

Downloaded 27 Jul 2011 to 140.116.71.27. Redistribution subject to ASME license or copyright; see http://www.asme.org/terms/Terms_Use.cfm

The extreme points of the Pareto set under uncertainty are shown to be the deterministic extreme points with a constant shift Δ when the set of active constraints remains unchanged. Therefore, the β-Pareto set of different P_f values can be easily predicted in the objective space. If we are able to calculate the value of failure probability that changes the constraint activity, denoted as P'_f, we can generalize the β-Pareto set by extending the deterministic Pareto generation method. In this algorithm, Lagrange multipliers associated with the active constraints are used to justify the value of P'_f when constraint activity changes. Details of the calculation of P'_f are shown in Sec. 2.3.

The process terminates when the failure probability ranges to be investigated are covered or when the failure probability value cannot be made smaller in the attainable set. The method proposed by Dauer and Liu for constructing BOLP in the objective space is introduced in Sec. 2.1. The shift of the Pareto set under uncertainty is discussed in Sec. 2.2. The method of using Lagrange multipliers to obtain P'_f is discussed in Sec. 2.3. A demonstration of the proposed method is given in Sec. 2.4.

2.1 Pareto Set Generation. To make this paper self-contained, this section describes the method of obtaining Pareto frontiers of the BOLP shown as [12]

$$\begin{aligned} &\min_{\mathbf{x}} \mathbf{f} = \mathbf{C}^T\mathbf{x} \\ &\text{subjectto } \mathbf{g} = \mathbf{A}^T\mathbf{x} - \mathbf{b} \le 0 \\ &\mathbf{x} \ge 0 \end{aligned} \tag{5}$$

Definition 2.1. *An extreme point* $\mathbf{f}_k^*$ *in the objective space is the optimum to the kth single-objective optimization problem defined as*

$$\mathbf{f}_k^* = [f_1(\mathbf{x}_k^*), \quad f_2(\mathbf{x}_k^*)], \quad \text{where } \mathbf{x}_k^* = \operatorname{argmin} f_k(\mathbf{x}), \quad \forall \mathbf{x} \in \mathcal{F} \tag{6}$$

Definition 2.2. *A design* $\bar{\mathbf{x}} \in \mathcal{F}$ *is said to be a vertex of* $\mathcal{F}$ *if there are no two distinct points* $\mathbf{x}_1$ *and* $\mathbf{x}_2$ *in* $\mathcal{F}$ *such that* $\bar{\mathbf{x}} = \alpha\mathbf{x}_1 + (1-\alpha)\mathbf{x}_2$ *for some* α, $0 < \alpha < 1$.

Definition 2.3. *A solution* $\bar{\mathbf{f}}$ *in a Pareto set* $\mathcal{P}$ *is said to be a vertex of* $\mathcal{P}$ *if there are no two distinct points* $\mathbf{f}_1$ *and* $\mathbf{f}_2$ *in* $\mathcal{P}$ *such that* $\bar{\mathbf{f}} = \alpha\mathbf{f}_1 + (1-\alpha)\mathbf{f}_2$ *for some* α, $0 < \alpha < 1$.

Definition 2.4. *For a* $k \times h$ *matrix,* $\boldsymbol{M}$ *denote the set of indices of the columns of* $\boldsymbol{M}$ *by* Id_M. *Hence, if* $\mathbf{M} = (\mathbf{m}^1, \mathbf{m}^2, \ldots, \mathbf{m}^h)$, *then* $Id_M = (1, 2, \ldots, h)$ *[12]. For a matrix* $\boldsymbol{M}$, *we define the positive cone spanned by the columns of* $\boldsymbol{M}$ *as*

$$\begin{aligned} \text{cone}(\mathbf{M}) &= \text{cone}(\mathbf{m}^i : i \in Id_M) \\ &= \left\{ \mathbf{m} \in \mathbb{R}^k : \mathbf{m} = \sum_{i \in Id_M} \alpha_i \mathbf{m}^i, \ \alpha_i \ge 0 \right\} \end{aligned}$$

Definition 2.5. *A frame,* F, *of cone* $\boldsymbol{M}$ *is a collection of columns of* $\boldsymbol{M}$ *such that* $\text{cone}(\mathbf{m}^i : i \in Id_F) = \text{cone}(\mathbf{M})$ and for each $j \in Id_F$, *we have* $\text{cone}(\mathbf{m}^i : i \in Id_F \backslash \{j\}) \neq \text{cone}(\mathbf{M})$ [12]

The method starts by generating extreme points of the Pareto frontier as the initial nondominant design. New vertexes of the Pareto frontier are then obtained from known extreme points until all extreme points are reached. Dauer and Liu showed that an edge of the feasible design space will map to an edge of the attainable set in the objective space if and only if the edge is a frame vector. Figure 3 illustrates the solution concept using a bi-objective linear problem. In what follows, we define a Pareto set of the BOLP in terms of its vertexes as

$$\mathcal{P} = \{\bar{\mathbf{f}}_1, \bar{\mathbf{f}}_2, \ldots, \bar{\mathbf{f}}_{n_v}\} \tag{7}$$

where n_v is the number of vertexes. As can be seen, the nondominated solutions of the attainable set form the Pareto set. Two

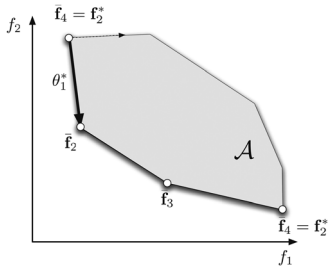

Fig. 3 Constructing the Pareto frontier of a BOLP

extreme points, $\mathbf{f}_1^*$ and $\mathbf{f}_2^*$, are obtained, with one being selected as the starting point to construct the entire Pareto frontier. Constraint activity at the selected extreme point, $\bar{y}_1$, is used to construct a reduced cost matrix $\mathbf{R}$. The elements of $\mathbf{R}$ are the vectors from $\bar{y}$'s mapped to the adjacent vertex in the design space, denoted as possible movement directions. The boundaries of $\mathbf{R}$ constitute the frame of possible movement directions that are obtained using a frame algorithm. Once the frame of $\mathbf{R}$ is available, the movement that satisfies Pareto frontier definition can be determined, shown as θ in Fig. 3. The largest step length in the given Pareto frame direction is calculated in an optimization subproblem as $\|\theta\|$. The new vertex in the Pareto frontier is then $\bar{\mathbf{f}}_2 = \bar{\mathbf{f}}_1 + \theta$. $\mathbf{f}_2$ is then used as the new extreme point to find the next vertex until $\mathbf{f}_2^*$ is reached. The detailed procedure of each step of the Pareto frontier construction is described below.

Step 1. Generate extreme points

In this step, Eq. (5) is considered as a collection of single-objective linear problems in Eq. (8), where $\mathbf{c}_k$ is the cost vector of the kth objective and $\mathbf{C} = [\mathbf{c}_1, \mathbf{c}_2]$. Equation (8) can be solved using the simplex method. Let the optimum be $\mathbf{x}_k^*$. $\mathbf{f}_k^* = \left[f_1(\mathbf{x}_k^*), f_2(\mathbf{x}_k^*)\right]$ will be one extreme point in the Pareto frontier. Since we focus on bi-objective problems only, the two extreme points are obtained as $\left[\mathbf{f}_1^*, \mathbf{f}_{22}^*\right]$

$$\begin{aligned} &\min_{\mathbf{x}} f_k = \mathbf{c}_k^T\mathbf{x} \\ &\text{subject to } \mathbf{g} = \mathbf{A}^T\mathbf{x} - \mathbf{b} \le 0 \\ &\mathbf{x} \ge 0 \end{aligned} \tag{8}$$

Step 2. Build reduced cost matrix

Once the extreme points are found in step 1, the corresponding active constraint set $\mathcal{K}_k$ for the kth objective in Eq. (8) is also known. An extreme point is selected as the starting point for Pareto frontier construction with the base variables being $\mathbf{x}_k^b$. The matrices $\mathbf{A}$ and $\mathbf{C}$ are then decomposed according to the base variables as

$$\begin{pmatrix} \mathbf{A} & \mathbf{b} \\ -\mathbf{C} & 0 \end{pmatrix} \rightarrow \begin{pmatrix} \mathbf{B} & \mathbf{D} & \mathbf{b} \\ -\mathbf{C}_B & -\mathbf{C}_D & 0 \end{pmatrix} \tag{9}$$

The reduced cost coefficient $\mathbf{R}$ that contains vectors of all directions from $\mathbf{x}_k^*$ to adjacent vertexes in the design space is then built using Eq. (10). The rank of $\mathbf{R}$ equals the problem dimension n.

$$\mathbf{R} = \mathbf{C}_B\mathbf{B}^{-1}\mathbf{D} - \mathbf{C}_D \tag{10}$$

Step 3. Determine the frame of R in the object space

Since $\mathbf{R}$ contains the vectors from $\mathbf{x}_k^*$ to the adjacent vertexes, not all their mappings to the objective space belong to the Pareto frontier. In this step, we adopt the frame algorithm from Ref. [13]

Downloaded 27 Jul 2011 to 140.116.71.27. Redistribution subject to ASME license or copyright; see http://www.asme.org/terms/Terms_Use.cfm

to obtain the frame of $\mathbf{R}$ in the objective space. The concept of the frame algorithm is that if the correct frame vectors are selected, the other vectors in $\mathbf{R}$ should be sums of the frame with positive coefficients. Let us now rewrite $\mathbf{R}$ as $[\mathbf{r}_1, \ldots, \mathbf{r}_n]$, where $\mathbf{r}_i$ has dimensions (2×1) and the set of all $\mathbf{r}$'s is $\mathcal{C}$. The set of frame candidates is $\mathcal{S}$, with two elements. The frame algorithm in Ref. [13] involves selecting candidates from $\mathcal{C}$ and then checking if all the coefficients $\mathbf{a}$ in Eq. (11) are non-negative. If a negative a is obtained, the current candidate cannot enclose all elements in $\mathcal{C}$ and therefore it is not a frame. In other words, the set of the frame of $\mathcal{C}$ must satisfy Eq. (11) with a non-negative $\mathbf{a}$.

$$\mathbf{r}_i = \sum_{j \in \mathcal{S}} a_j \mathbf{r}_j, \quad i \in (\mathcal{C} - \mathcal{S}) \tag{11}$$

Step 4. Determine a Pareto frame vector

After the frame vectors are obtained in step 3, only the frame vector with the most improved objective function values forms the Pareto set. Figure 4 shows a cone spanned by the vectors $\mathbf{r}_1$ and $\mathbf{r}_2$ in the $(f_1 - f_2)$ space. Since both objective functions are to be minimized, $\mathbf{r}_2$ is dominated by $\mathbf{r}_1$ since the projection of the unit vector of $\mathbf{r}_1$ onto f_1, denoted as $(\mathbf{r}_1/\|\mathbf{r}_1\|)_{f_1}$, and that of $\mathbf{r}_2$ satisfy

$$\left(\frac{\mathbf{r}_1}{\|\mathbf{r}_1\|}\right)_{f_1} \leq \left(\frac{\mathbf{r}_2}{\|\mathbf{r}_2\|}\right)_{f_1} \tag{12}$$

Step 5. Find the step length of the Pareto frame vector

Once the Pareto frame vector is obtained, points along the frame belong to the Pareto frontier until they are no longer in the attainable set. The maximal length of the step vector can be found using

$$\begin{gathered} \max_{\mathbf{x},\theta} \theta \\ \text{subject to } \mathbf{C}^T\mathbf{x} + \theta\mathbf{r} = \bar{\mathbf{f}}_i \\ \mathbf{A}^T\mathbf{x} - \mathbf{b} \leq 0 \\ \theta, \mathbf{x} \geq 0 \end{gathered} \tag{13}$$

Step 6. Iterate until the termination condition is reached

The updated extreme point is $\bar{\mathbf{f}}_2 = \bar{\mathbf{f}}_1 + \theta^*\mathbf{r}$. The optimal $\mathbf{x}$ of Eq. (13) is the vertex. The activity of $\bar{\mathbf{f}}_2$ is also known. Repeat steps 2–6 until termination condition is reached.

2.2 Shift of Pareto Sets. Each vertex in the objective space has a corresponding vertex at a different P_f value. We prove that the values of P_f directly affect the feasible space of the probabilistic constraints in Sec. A.2 of the Appendix. Assuming that the active constraint set remains unchanged, the matrix $\mathbf{R}$ will be the same and therefore the original frame direction will not be changed. Consider active constraints as equalities with the intersections being the vertexes in the design space. From Sec A.3 of the Appendix, we know that the constraint boundaries change with P_f. The new vertexes at a different P_f are then the result of a shift of the original vertexes along the direction given in Eq. (14). By connecting the shifted vertexes, we obtain the β-Pareto set in the objective space

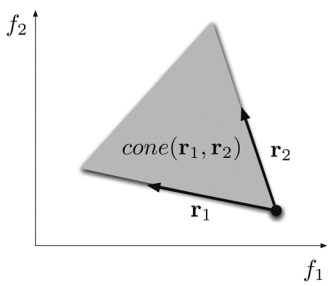

Fig. 4 Cone of a Pareto frame

$$\begin{gathered} \bar{\mathbf{f}}_{\text{new}} = \bar{\mathbf{f}} + \mathbf{z} \\ \text{where } \mathbf{z} = \mathbf{C}^T\mathbf{A}^{-1}\Delta = \mathbf{C}^T\mathbf{A}^{-1}\boldsymbol{\sigma}_g\Phi(1 - P_f) \end{gathered} \tag{14}$$

2.3 Constraint Activity Prediction at Different P_f. Section 2.2 described how to construct the β-Pareto set assuming that the constraint activities are unchanged when P_f varies. These methods are applicable when the constraint activities changes. Algorithmically, an active set of constraints can be identified via Lagrange multiplier estimated values $\boldsymbol{\lambda}$. However, obtaining Lagrange multipliers of probabilistic constraints is difficult in practice because G_j is hard to calculate globally for nonlinear functions, if at all possible. Fortunately, the neighborhood of a design point G_j can be approximated locally using the first order reliability method [14]. The true $\boldsymbol{\lambda}$ is only computed at the optimum, so the Lagrange multipliers are only estimates in the intermediate iterations. In an active set strategy, as $k \to \infty$ (or in practice, as iterations proceed), $\boldsymbol{\mu}_{\mathbf{X}}^k \to \boldsymbol{\mu}_{\mathbf{X}}^*$, the multiplier estimates approach the true ones, $\boldsymbol{\lambda}^k \to \boldsymbol{\lambda}^*$, and the working set $\mathcal{G}^k$ becomes the true active set $\mathcal{G}^*$.

Lemma 1. *The change of $\mathcal{F}$ due to P_f can be observed from the vertex in the design space.*

Proof. This can be proved by contradiction. If a feasible space is altered without changing any vertexes, $\mathcal{F}$ will not be a polyhedral, which violates the basic principle of LP problems.

Lemma 2. *The change of $\mathcal{P}$ due to P_f can be observed from the vertex in the objective space.*

Proof. When the change of $\mathcal{F}$ is mapped onto the objective space, one of the following cases will occur:

The new vertexes do not change $\mathcal{P}$; the corner points of $\mathcal{P}$ will not have any effects.
The vertexes map onto $\mathcal{P}$ as corner points.
The vertexes map onto $\mathcal{P}$ as segments between corner points.

The corner points can thus be used to obtain the correct information of constraint activity change.

Theorem 3.1 in Ref. [12] shows that the edge in a design space will be mapped as an edge in the corresponding objective space only if the vector is in the frame. In this work, we extend the concept and connect the shifted vertexes to obtain the shifted edge in the Pareto set in the objective space. Combining Lemmas 1 and 2 yields the following theorem:

Theorem 1. *For an LP problem, any change in constraint activity can be observed at the vertex.*

In this research, we use Theorem 1 to determine the critical failure probability level P_f' that changes the active constraint set as the solution to Eq. (15), where $\lambda_{f,j}$ is the Lagrange multiplier for constraint g_j at a given failure probability level P_f. This method only requires the Lagrange multipliers at the vertexes

$$\begin{gathered} \min_{P_f} P_f \\ \text{s.t.} \lambda_{f,j} - \lambda_j' = 0 \\ j = 1, \ldots, m \end{gathered} \tag{15}$$

2.4 Demonstration. In this section, we use the bi-objective optimization problem in Eq. (16) to demonstrate how the β-Pareto set can be obtained analytically for LP problems using the proposed approach. The original deterministic formulation in Ref. [12] is modified such that all design variables are random with $\boldsymbol{\sigma}_{\mathbf{X}} = 1$.

Table 1 shows the nondominant points of the deterministic Pareto set as calculated via the approach presented in Sec. 2.1. The reduced cost coefficient matrix of each nondominant solution and the corresponding frame vectors are also listed. The maximum step length θ along each frame vector is obtained. Figure 5 shows the deterministic Pareto set and the β-Pareto set. As can be seen, the deterministic Pareto set can be formed by connecting nondominant vertex design points $\bar{\mathbf{f}}_1$, $\bar{\mathbf{f}}_2$, $\bar{\mathbf{f}}_3$, and $\bar{\mathbf{f}}_4$

Downloaded 27 Jul 2011 to 140.116.71.27. Redistribution subject to ASME license or copyright; see http://www.asme.org/terms/Terms_Use.cfm

Table 1 Vertexes of the β-Pareto set of Eq. (16)

	R			Frame of R	θ
$\bar{\mathbf{f}}_1 = \begin{pmatrix} -8.11 \\ -0.11 \end{pmatrix}$	$\begin{pmatrix} 0.014 & 0.002 & 0.889 \\ -0.004 & -0.143 & -0.111 \end{pmatrix}$			$\begin{pmatrix} 0.002 \\ -0.143 \end{pmatrix}$	0.789
$\bar{\mathbf{f}}_2 = \begin{pmatrix} -8.10 \\ -0.90 \end{pmatrix}$	$\begin{pmatrix} -0.002 & 0.014 & 0.900 \\ 0.113 & -0.014 & -0.900 \end{pmatrix}$			$\begin{pmatrix} 0.014 \\ -0.014 \end{pmatrix}$	10.182
$\bar{\mathbf{f}}_3 = \begin{pmatrix} -0.90 \\ -8.10 \end{pmatrix}$	$\begin{pmatrix} 0.113 & -0.014 & -0.900 \\ -0.002 & 0.014 & 0.900 \end{pmatrix}$			$\begin{pmatrix} 0.113 \\ -0.002 \end{pmatrix}$	0.789
$\bar{\mathbf{f}}_4 = \begin{pmatrix} -0.11 \\ -8.11 \end{pmatrix}$	$\begin{pmatrix} -0.004 & -0.143 & 0.111 \\ 0.014 & 0.002 & 0.889 \end{pmatrix}$				
$\bar{\mathbf{f}}_5 = \begin{pmatrix} -7.57 \\ -0.71 \end{pmatrix}$	$\begin{pmatrix} -0.13 & 0.00 & -0.16 \\ 0.02 & 0.00 & 0.16 \end{pmatrix}$			$\begin{pmatrix} -0.13 \\ 0.02 \end{pmatrix}$	9.71
$\bar{\mathbf{f}}_6 = \begin{pmatrix} -0.71 \\ -7.57 \end{pmatrix}$	$\begin{pmatrix} 0.02 & 0.00 & 0.16 \\ -0.13 & 0.00 & -0.16 \end{pmatrix}$				

$$
\begin{aligned}
\min_{\boldsymbol{\mu}_\mathbf{X}} \mathbf{c}^T \boldsymbol{\mu}_\mathbf{X} &= \begin{pmatrix} -\boldsymbol{\mu}_{X_1} - 1/9\mu_{X_3} \\ -\boldsymbol{\mu}_{X_2} - 1/9\mu_{X_3} \end{pmatrix} \\
\text{s.t.} \Pr[g_1 = 9X_1 + 9X_2 + 2X_3 - 81 > 0] &\le P_\mathrm{f} \\
\Pr[g_2 = 8X_1 + X_2 + 8X_3 - 72 > 0] &\le P_\mathrm{f} \\
\Pr[g_3 = X_1 + 8X_2 + 8X_3 - 72 > 0] &\le P_\mathrm{f} \\
\Pr[g_4 = -7X_1 - X_2 - X_3 + 9 > 0] &\le P_\mathrm{f} \\
\Pr[g_5 = -X_1 - 7X_2 - X_3 + 9 > 0] &\le P_\mathrm{f} \\
\Pr[g_6 = -X_1 - X_2 - 7X_3 + 9 > 0] &\le P_\mathrm{f} \\
\Pr[g_7 = X_1 - 8 > 0] &\le P_\mathrm{f} \\
\Pr[g_8 = X_2 - 8 > 0] &\le P_\mathrm{f} \\
\mathbf{X} &\sim N(\boldsymbol{\mu}_\mathbf{X}, \boldsymbol{\sigma}_\mathbf{X}^2)
\end{aligned}
\tag{16}
$$

Table 2 lists the limit of failure probability without changing the activity for each constraint. At the deterministic optimum for $P_\mathrm{f} = 50\%$, constraints g_2 and g_7 are active at $\bar{\mathbf{f}}_1$. The projections of $\mathbf{CA}^{-1}\boldsymbol{\Delta}$ on objective functions provide the movement directions of vertexes with increasing reliability. As can be seen, at a reliability value of 69.3%, points $\bar{\mathbf{f}}_1$ and $\bar{\mathbf{f}}_2$ merge into point $\bar{\mathbf{f}}_5$, and points $\bar{\mathbf{f}}_3$ and $\bar{\mathbf{f}}_4$ merge into point $\bar{\mathbf{f}}_6$. The maximal reliability in the probabilistic design space of Eq. (16) is 98.3% when points $\bar{\mathbf{f}}_5$ and $\bar{\mathbf{f}}_6$ merge into point $\bar{\mathbf{f}}_7$.

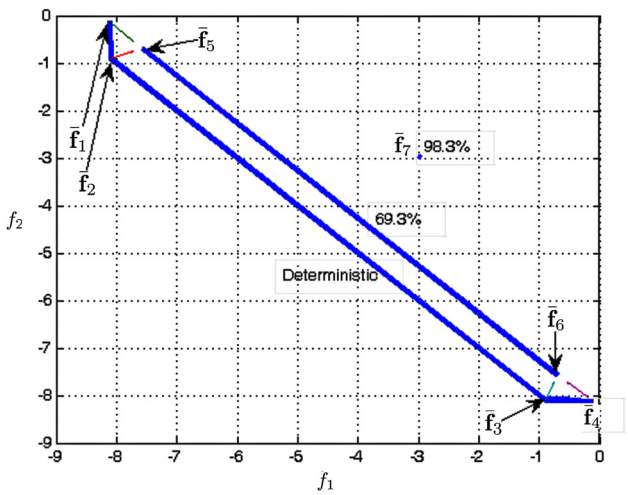

Fig. 5 β-Pareto set of Eq. (16)

Table 2 Relations between vertexes of the β-Pareto set

Vertex point	$\bar{\mathbf{f}}_1$	$\bar{\mathbf{f}}_2$	$\bar{\mathbf{f}}_3$	$\bar{\mathbf{f}}_4$	$\bar{\mathbf{f}}_5$	$\bar{\mathbf{f}}_6$
$\mathbf{CA}^{-1}\boldsymbol{\Delta}$ on f_1	1.064	1.042	0.390	− 1.181	2.834	− 1.403
$\mathbf{CA}^{-1}\boldsymbol{\Delta}$ on f_2	− 1.181	0.390	1.042	1.064	− 1.403	2.834
Minimum reliability (%)	50.0	50.0	50.0	50.0	69.3	69.3
Maximum reliability (%)	69.3	69.3	69.3	69.3	98.3	98.3

Figure 5 is a useful tool for decision-making when the trade-offs between reliability and performance measures are considered. For the deterministic Pareto set, we have the standard trade-off information between f_1 and f_2. If the reliability is to be increased, the decision-maker can immediately know how the decision affects reliability. For example, if one would like to know the trade-offs between f_1 and f_2 when the constraint reliability is 95%, one can simply connect $\bar{\mathbf{f}}_5$ and $\bar{\mathbf{f}}_6$ with $\bar{\mathbf{f}}_7$ and use Eq. (14) to obtain the shifted Pareto set. The result will show that the Pareto set of f_1 and f_2 at 95% reliability is

$$
\mathcal{P}_{95\%} = \left\{ \begin{pmatrix} -4.34 \\ -2.31 \end{pmatrix}, \begin{pmatrix} -2.31 \\ -4.34 \end{pmatrix} \right\}
$$

3 Bi-Objective Nonlinear Programming Under Uncertainty

The β-Pareto set generated via the approach presented in Sec. 2 is exact for BOLP problems. However, this method faces several challenges for bi-objective nonlinear programming (BONLP) problems under uncertainty:

(1) The deterministic Pareto set of a BONLP problem does not have exact forms. Only a limited number of Pareto points are available in general engineering applications;
(2) The constraint activities in BONLP are much more complex and the theorems for predicting constraint boundary shifts for BOLP might not be applicable;
(3) When constraints are nonlinear, using the first order concept for estimating constraint boundary shifts might not be accurate.

These challenges are overcome by extending the BOLP method to nonlinear problems. We use the minimum number of Pareto points to ensure efficiency by obtaining important Pareto points that need to be verified with real simulations. We also use an algorithm to identify the threshold values of P_f when the constraint activity changes. We ensure that the accuracy of the resulting β-Pareto set is at the level request by the designer. Details of the implementation are given below.

To extend the method for LP problems to NLP, we assume that BONLP problems can be approximated by a finite set of BOLP problems. In other words, the attainable set $\mathcal{A}$ of a BONLP problem is the sum of the attainable sets $\hat{\mathcal{A}}_k$ of a finite set of BOLP subproblems, as shown in Eq. (17). If the BONLP is highly nonlinear, one needs to use a large number of $\hat{\mathcal{A}}_k$ sets to ensure accuracy

$$
\mathcal{A} \approx \sum_{\forall k} \hat{\mathcal{A}}_k \tag{17}
$$

Downloaded 27 Jul 2011 to 140.116.71.27. Redistribution subject to ASME license or copyright; see http://www.asme.org/terms/Terms_Use.cfm

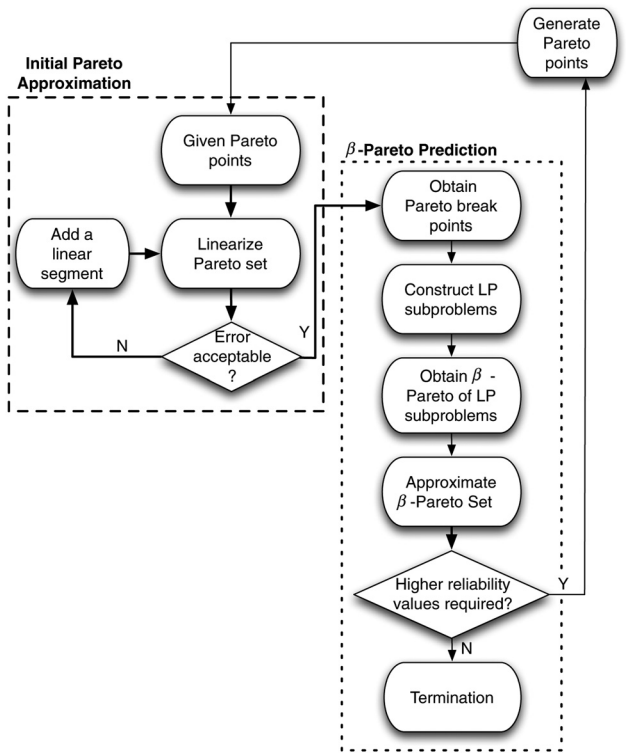

Fig. 6 Flowchart for predicting β-Pareto set for BONLP

Equation (17) is used to approximate a Pareto set $(\mathcal{P})$ via a finite set of linear segments $(\hat{\mathcal{P}}_k)$ such that $\mathcal{P} \approx \sum_{\forall k} \hat{\mathcal{P}}_k$.

Figure 6 shows the two-stage process flow of the proposed method for constructing the β-Pareto set of a BONLP under uncertainty. The first stage is the initial Pareto set approximation that uses a sandwich method to obtain the linear segmentations of the Pareto set. The upper and the lower bounds of the approximation result in an error measure. If the error is higher than a predetermined value E^s, an additional line segment is added to the Pareto approximation. The quality of the representation of the original NLP space and the accuracy of the final β-Pareto approximation increase with increasing number of linear segments. This stage converges when the error of the sandwich Pareto approximation is acceptable.

The first stage of Fig. 6 provides the linear segments of the Pareto set and the linearization points. These break points are then used to linearize BONLP problems. Assuming that n_b break points are created, we have n_b BOLP subproblems. Each of these BOLP subproblems results in a β-Pareto set obtained using the β-Pareto generation method presented in Sec. 2. We can then construct the approximation of the BONLP β-Pareto set by combining a number of BOLP β-Pareto sets. This β-Pareto approximation is only accurate at a certain reliability level within the given tolerances. If a reliability value higher than the current limit is desired, new Pareto points of the original BONLP are generated. This process continues until either the maximum reliability is reached or the obtained reliability is sufficiently high.

The details of the steps in Fig. 6 are described below using the mathematical example shown in Eq. (18). Two nonlinear objectives are minimized in Eq. (18) with the probabilistic feasible space defined by two nonlinear constraints. The proposed approach first assumes that n_p Pareto points have been generated without knowing the entire deterministic Pareto set. This is a practical assumption, as in most engineering problems, only a finite set of Pareto points are used to represent the entire set

$$\begin{aligned} \min_{\boldsymbol{\mu}_\mathbf{X}} f(\boldsymbol{\mu}_\mathbf{X}) &= \begin{pmatrix} -\mu_{X_1}\mu_{X_2} + 5 \\ 0.5\mu_{X_1}\mu_{X_3} + 50 \end{pmatrix} \\ \text{s.t.} \Pr[X_1^2 + 0.1X_2^2 - X_3 - 50 > 0] &\le P_\text{f} \\ \Pr[0.1X_1^2 + 0.4X_2^2 + X_3 > 0] &\le P_\text{f} \\ \forall \mathbf{X} &\sim N(\boldsymbol{\mu}_\mathbf{X}, \boldsymbol{\sigma}_\mathbf{X}^2), \\ \text{where } \boldsymbol{\mu}_\mathbf{X} &\le 0, \boldsymbol{\sigma}_\mathbf{X} = 1 \end{aligned} \tag{18}$$

3.1 Sandwich Method in Pareto Set Approximation. In this section, we describe the sandwich approach for approximating the Pareto set as linear segments based on the n_p Pareto points available. The upper and lower bound approximations of a Pareto set in Ref. [15] start with the connection of the optimal point of each objective function to form a two dimensional hyperplane. Let the Pareto set be partitioned into n segments. The upper bound function u_i of the ith segment is expressed as

$$u_i = f_2^i + \frac{f_2^{i+1} - f_2^i}{f_1^{i+1} - f_1^i}(f_1 - f_1^i), \ \forall f_1 \in [f_1^i, f_1^{i+1}] \tag{19}$$

Define $e_i = \frac{f_2^{i+1} - f_2^i}{f_1^{i+1} - f_1^i}$ as the slope of the upper bound function. The lower bound function l_i can then be found as the function parallel to u_i with the maximum distance between them while remaining in contact with at least one Pareto point. Equation (20) shows the concept, where $f_1^{i\prime}$ is the tangent point of the function l_i to the Pareto set

$$\begin{aligned} l_i &= f_2^{i\prime} + e_i(f_1 - f_1^{i\prime}) \\ \text{where } f_1^{i\prime} &= \arg\min\{f_2 - e_i f_1, \forall f_1^i \le f_1 \le f_1^{i+1}\} \end{aligned} \tag{20}$$

The upper and lower bound approximations, u_i and l_i, contain the true Pareto set. The more Pareto points available, the higher the accuracy of this approximation can be. The maximum number of segments is n_p and the minimum number is 1. The distance between u_i and l_i is an index for approximation accuracy, denoted as E^s.

In this study, we use the values of one objective within u_i and l_i to be the measure of the Pareto approximation error. For a bi-objective problem, Eq. (21) uses the values of f_2 within the bounds, Δf_2, as the error of the sandwich approximation, as shown in Fig. 7. If the objective function variation is not acceptable, more linear segments should be added until $\Delta f_2 \le E^s$.

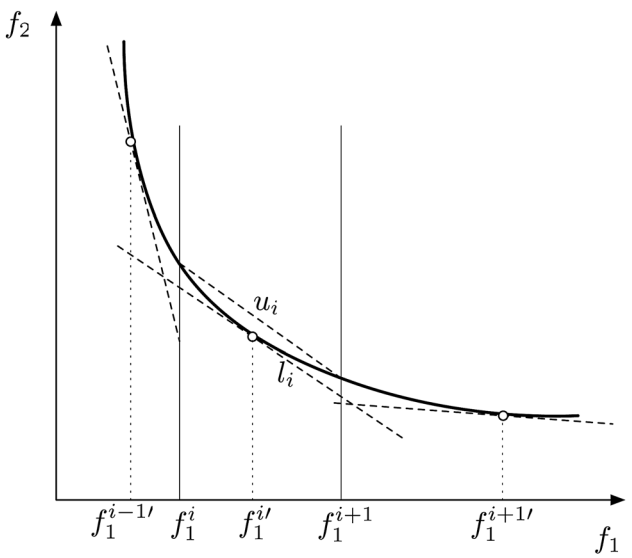

Fig. 7 Sandwich approach in Pareto approximation

Downloaded 27 Jul 2011 to 140.116.71.27. Redistribution subject to ASME license or copyright; see http://www.asme.org/terms/Terms_Use.cfm

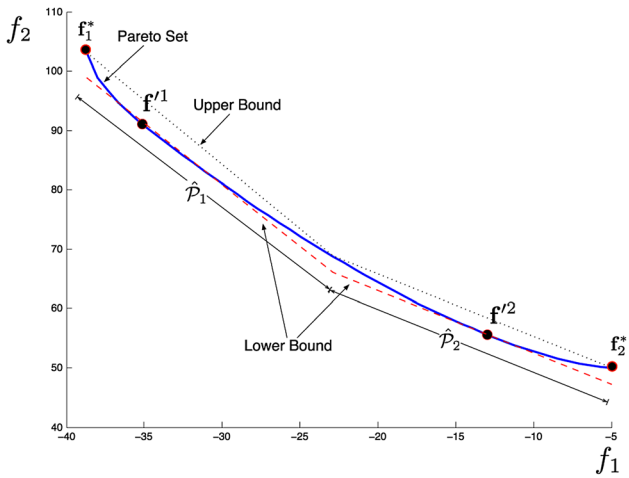

Fig. 8 Linear segmentation of Eq. (18)

$$\Delta f_2 = \max_i \{u_i(f_1^{i\prime}) - l_i(f_1^{i\prime})\} \tag{21}$$

Figure 8 shows the results of the sandwich approximation to Eq. (18) with $E^s = 3$. As can be seen, two piecewise linear segments are obtained with breakpoints $\mathbf{f}^{1\prime} = [-35.13,\ 91.09]$ and $\mathbf{f}^{2\prime} = [-12.96,\ 55.58]$. We use a large E^s to show the upper and lower bounds. A much better approximation can be obtained by increasing the number of linear segments.

3.2 Linear Subproblems in Pareto Approximation. The attainable set of the original nonlinear problem is approximated as the sum of a finite number of linear attainable sets, as in Eq. (17). The sandwich method presented in Sec. 3.1 helps to determine the number of required linear sets for approximating the Pareto set. The corresponding linear subproblems in each attainable set approximate are presented in this section. Let $\mathbf{f}'$ be the linearization point in the objective space. In this step, we map the linearization point to the design space and find the corresponding linear boundaries of active constraints. The linearization point in the design space, $\mathbf{x}'$, can be found using the constraint method in the objective space. In Fig. 7, we have $\mathbf{f}^i$ as the linear segments in the objective space. The corresponding linear design point $\mathbf{x}'$ can then be found as the solution to

$$\begin{aligned} &\min_{\mathbf{x}} f_2(\mathbf{x}) \\ &\text{s.t. } f_1(\mathbf{x}) = f_1'^i \\ &\forall \mathbf{x} \in \mathcal{F} \end{aligned} \tag{22}$$

Once the linearization point in the design space ($\mathbf{x}'$) is found, the corresponding LP subproblem with respect to $\mathbf{x}'$ can be obtained as

$$\text{LP}(\mathbf{x}'): \begin{cases} \min\limits_{\mathbf{x}} & \hat{\mathbf{f}}(\mathbf{x}) = \mathbf{C}_f^T \mathbf{x} \\ \text{s.t.} & \mathcal{F}' = \{\hat{\mathbf{g}} = \mathbf{A}^T \mathbf{x} \le \mathbf{B},\ \mathbf{g}_a = \mathbf{A}_a^T \mathbf{x} \le \mathbf{B}_a\} \end{cases}$$

where $\mathbf{C}_f^T = \nabla \mathbf{f}|_{\mathbf{x}=\mathbf{x}'}$, $\mathbf{A}^T = \nabla \mathbf{g}|_{\mathbf{x}=\mathbf{x}'}$, and $\mathbf{B} = \mathbf{g}|_{\mathbf{x}=\mathbf{x}'} - \nabla \mathbf{g}|_{\mathbf{x}=\mathbf{x}'} \cdot \mathbf{x}'$. The feasible space $\mathcal{F}'$ in LP ($\mathbf{x}'$) considers not only the linearization of the original constraints, $\hat{g}$, but also auxiliary constraints, denoted as $\mathbf{g}_a$, to ensure that the design will not go beyond the extreme points in the original Pareto set. These auxiliary constraints ensure that the design matches the original extreme conditions, thus improving the accuracy of the Pareto set approximation. $\mathbf{A}_a$ and $\mathbf{B}_a$ are obtained by identifying the extreme points $\mathbf{x}^*$ in the design space and linearizing the constraints at these points. Therefore, $\mathbf{A}_a = \nabla \mathbf{g}|_{\mathbf{x}^*=\mathbf{x}^*}$, and $\mathbf{B}_a = \mathbf{g}|_{\mathbf{x}=\mathbf{x}^*} - \nabla \mathbf{g}|_{\mathbf{x}=\mathbf{x}^*} \cdot \mathbf{x}^*$. Table 3 lists the results of two LP subproblems generated at break points $\mathbf{f}'^1$ and $\mathbf{f}'^2$.

3.3 Approximate β-Pareto Set. The solutions to each BOLP subproblem are then obtained using the method described in Sec. 2. Different from the LP case, the minimum failure probability of a Pareto set shifting depends not only on constraint activities but also on the accuracy of the shift. This is calculated by comparing the true Pareto points using the constraint method with the Pareto approximation when all objective functions are fixed but one, as shown in Eq. (23). The objective function in Eq. (23) is to obtain the maximum reliability (minimum failure probability) while the Pareto set prediction for another objective $\hat{f}_2$ is within acceptable range E^p from the true Pareto b using the constraint method

$$\begin{aligned} &\min_{a,P_f} P_f \\ &\text{s.t.} |\hat{f}_2 - b|/\hat{f}_2 \le E^p \\ &a \in \{\hat{f}_1^k, \hat{f}_1^{k+1}\}, P_f \in \{0, 50\%\} \\ &b = \min f_2, \mathbf{x} \in \mathcal{F}, f_1 \le a \end{aligned} \tag{23}$$

For $E^p = 5\%$, Fig. 9 shows the β-Pareto set of Eq. (18) obtained using the proposed method. Table 4 lists the vertexes of these β-Pareto sets. As can be seen, the deterministic Pareto set approximated via two break points is valid only between $P_f = 50\%$ and $P_f = 41\%$ due to the highly nonlinear nature of the problem even though $\hat{\mathcal{P}}^0$ in Table 4 shows that the constraint activity will remain unchanged until $P_f = 2\%$. A new Pareto approximation $\hat{\mathcal{P}}^1$ is then generated that is valid for P_f values between 41% and 33%. Likewise, $\hat{\mathcal{P}}^2$ is valid for P_f values between 33% and 9% and $\hat{\mathcal{P}}^3$ is valid for P_f values between 9% and 3%.

Based on these results, if one is interested in the trade-offs between objective functions at a reliability level within [67%, 91%], $\hat{\mathcal{P}}^2$ and $\hat{\mathcal{P}}^3$ can be used. For example

Table 3 Pareto set approximation of Eq. (18)

Break point on $\mathcal{P}$	$\mathbf{f}^{1\prime} = \begin{pmatrix} -35.13 \\ 91.09 \end{pmatrix}$	$\mathbf{f}^{2\prime} = \begin{pmatrix} -12.96 \\ 55.58 \end{pmatrix}$
Linear design point	$\mathbf{x}^{1\prime} = (-5.74, -5.25, -14.33)$	$\mathbf{x}^{2\prime} = (-3.03, -2.63, -3.68)$
$\mathbf{C}_f$ in LP ($\mathbf{x}'$)	$\begin{pmatrix} 4.97 & 5.34 & 0 \\ -7.26 & 0 & -2.67 \end{pmatrix}$	$\begin{pmatrix} 2.56 & 2.79 & 0 \\ -2.19 & 0 & -1.39 \end{pmatrix}$
$\mathbf{A}$ in LP ($\mathbf{x}'$)	$\begin{pmatrix} -11.47 & -1.05 & -1.00 \\ -1.15 & -4.2 & 1.00 \end{pmatrix}$	$\begin{pmatrix} -6.06 & -0.53 & -1.00 \\ -0.61 & -2.10 & 1.00 \end{pmatrix}$
$\mathbf{B}$ in LP ($\mathbf{x}'$)	$(85.67, 14.33)^T$	$(59.88, 3.68)^T$
$\mathbf{A}_a$ in LP ($\mathbf{x}'$)	$\begin{pmatrix} -9.53 & -1.41 & -1.00 \\ -0.95 & -5.66 & 1.00 \\ 0.00 & -0.16 & -1.00 \\ 0.00 & -0.65 & 1.00 \end{pmatrix}$	
$\mathbf{B}_a$ in LP ($\mathbf{x}'$)	$(77.73, 22.27, 50.07, 0.26)^T$	

Downloaded 27 Jul 2011 to 140.116.71.27. Redistribution subject to ASME license or copyright; see http://www.asme.org/terms/Terms_Use.cfm

$$\hat{\mathcal{P}}_{80\%} = \left\{ \begin{pmatrix} -32.06 \\ 98.83 \end{pmatrix}, \begin{pmatrix} -29.05 \\ 88.44 \end{pmatrix}, \begin{pmatrix} -15.77 \\ 61.52 \end{pmatrix}, \begin{pmatrix} -9.06 \\ 53.37 \end{pmatrix}, \begin{pmatrix} -1.07 \\ 45.83 \end{pmatrix} \right\}$$

and

$$\hat{\mathcal{P}}_{85\%} = \left\{ \begin{pmatrix} -30.39 \\ 98.00 \end{pmatrix}, \begin{pmatrix} -27.15 \\ 86.84 \end{pmatrix}, \begin{pmatrix} -13.92 \\ 60.01 \end{pmatrix}, \begin{pmatrix} -8.52 \\ 53.46 \end{pmatrix}, \begin{pmatrix} -1.28 \\ 46.04 \end{pmatrix} \right\}$$

If a higher reliability is needed, one might use $\hat{\mathcal{P}}^3$ to get

$$\hat{\mathcal{P}}_{95\%} = \left\{ \begin{pmatrix} -27.25 \\ 95.98 \end{pmatrix}, \begin{pmatrix} -21.49 \\ 80.17 \end{pmatrix}, \begin{pmatrix} -12.10 \\ 60.34 \end{pmatrix}, \begin{pmatrix} -5.84 \\ 50.44 \end{pmatrix}, \begin{pmatrix} -0.33 \\ 45.00 \end{pmatrix} \right\}$$

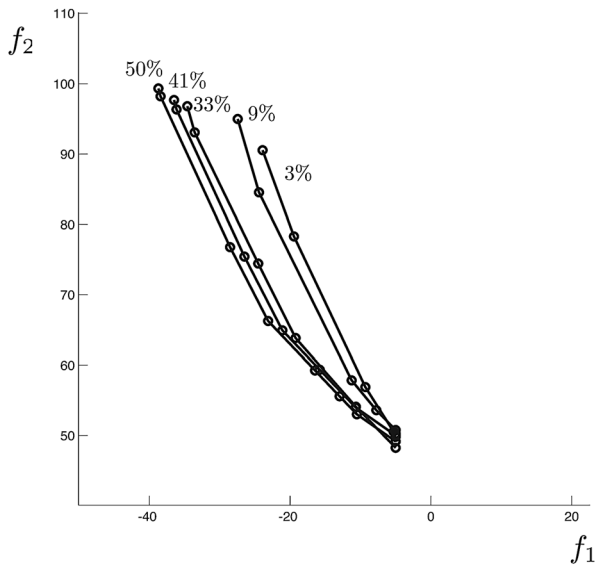

Fig. 9 β-Pareto set approximation of Eq. (18)

These results have the accuracy levels of E^s and E^p and can readily be available without running additional optimization routines.

4 Multi-Objective Design of Vehicle Crashworthiness

The multi-objective optimal vehicle design considering occupant safety from Refs. [16,17] under uncertainty is studied using the proposed method. Two objectives of interest are minimizing the overall weight of the vehicle and optimizing the index for the side impact test (i.e., the door intrusion velocity). These two objectives contradict each other in that upgrading the body side helps to reduce the severity of the subsequent momentum exchange between the door and the occupant but increases the weight. In addition to the objective functions, constraints on other design considerations are to be satisfied with high reliability values under operational and material uncertainties. Equation (24) shows the problem formulation of the crashworthiness study. The surrogate models created by Gu et al. [16] are used to replace the computationally expensive finite element models.

4.1 Problem Description. The vehicle design problem is formulated as Eq. (24), with two objective functions, nine con-

Table 4 Vertexes of the β-Pareto approximation of Eq. (18)

$$\hat{\mathcal{P}}_1^0 : \left\{ \begin{pmatrix} -38.80 \\ 99.68 \\ 2\% \end{pmatrix}, \begin{pmatrix} -38.41 \\ 98.20 \\ 2\% \end{pmatrix}, \begin{pmatrix} -28.52 \\ 76.76 \\ 2\% \end{pmatrix}, \begin{pmatrix} -3.94 \\ 28.90 \\ 2\% \end{pmatrix} \right\}$$

$$\hat{\mathcal{P}}_2^0 : \left\{ \begin{pmatrix} -36.61 \\ 118.94 \\ 13\% \end{pmatrix}, \begin{pmatrix} -35.33 \\ 108.83 \\ 2\% \end{pmatrix}, \begin{pmatrix} -30.04 \\ 82.12 \\ 2\% \end{pmatrix}, \begin{pmatrix} -29.82 \\ 81.20 \\ 5\% \end{pmatrix}, \begin{pmatrix} -24.42 \\ 67.61 \\ 2\% \end{pmatrix}, \begin{pmatrix} -16.46 \\ 59.25 \\ 2\% \end{pmatrix}, \begin{pmatrix} -12.96 \\ 55.58 \\ 20\% \end{pmatrix}, \begin{pmatrix} -10.51 \\ 53.00 \\ 1\% \end{pmatrix}, \begin{pmatrix} 1.74 \\ 44.42 \\ 41\% \end{pmatrix} \right\}$$

$$\hat{\mathcal{P}}_1^1 : \left\{ \begin{pmatrix} -37.14 \\ 100.39 \\ 2\% \end{pmatrix}, \begin{pmatrix} -35.57 \\ 94.73 \\ 2\% \end{pmatrix}, \begin{pmatrix} -26.32 \\ 75.66 \\ 2\% \end{pmatrix}, \begin{pmatrix} -2.93 \\ 28.91 \\ 2\% \end{pmatrix} \right\}$$

$$\hat{\mathcal{P}}_2^1 : \left\{ \begin{pmatrix} -34.55 \\ 115.19 \\ 2\% \end{pmatrix}, \begin{pmatrix} -33.59 \\ 107.05 \\ 2\% \end{pmatrix}, \begin{pmatrix} -28.73 \\ 82.85 \\ 2\% \end{pmatrix}, \begin{pmatrix} -27.88 \\ 79.32 \\ 2\% \end{pmatrix}, \begin{pmatrix} -22.91 \\ 67.27 \\ 2\% \end{pmatrix}, \begin{pmatrix} -11.21 \\ 53.99 \\ 2\% \end{pmatrix}, \begin{pmatrix} -3.30 \\ 45.79 \\ 2\% \end{pmatrix} \right\}$$

$$\hat{\mathcal{P}}_1^2 : \left\{ \begin{pmatrix} -35.47 \\ 100.63 \\ 4\% \end{pmatrix}, \begin{pmatrix} -32.79 \\ 91.91 \\ 2\% \end{pmatrix}, \begin{pmatrix} -3.86 \\ 32.78 \\ 2\% \end{pmatrix} \right\}$$

$$\hat{\mathcal{P}}_2^2 : \left\{ \begin{pmatrix} -32.48 \\ 111.28 \\ 2\% \end{pmatrix}, \begin{pmatrix} -31.79 \\ 104.86 \\ 2\% \end{pmatrix}, \begin{pmatrix} -27.42 \\ 83.27 \\ 2\% \end{pmatrix}, \begin{pmatrix} -26.01 \\ 77.61 \\ 2\% \end{pmatrix}, \begin{pmatrix} -21.47 \\ 67.04 \\ 2\% \end{pmatrix}, \begin{pmatrix} -10.06 \\ 53.05 \\ 2\% \end{pmatrix}, \begin{pmatrix} -2.52 \\ 45.33 \\ 2\% \end{pmatrix} \right\}$$

$$\hat{\mathcal{P}}_1^3 : \left\{ \begin{pmatrix} -29.65 \\ 97.66 \\ 2\% \end{pmatrix}, \begin{pmatrix} -24.14 \\ 82.61 \\ 2\% \end{pmatrix}, \begin{pmatrix} -0.24 \\ 32.10 \\ 2\% \end{pmatrix} \right\}$$

$$\hat{\mathcal{P}}_2^3 : \left\{ \begin{pmatrix} -25.15 \\ 93.86 \\ 2\% \end{pmatrix}, \begin{pmatrix} -22.75 \\ 82.01 \\ 2\% \end{pmatrix}, \begin{pmatrix} -20.29 \\ 73.10 \\ 2\% \end{pmatrix}, \begin{pmatrix} -17.18 \\ 67.19 \\ 2\% \end{pmatrix}, \begin{pmatrix} -6.53 \\ 50.28 \\ 2\% \end{pmatrix}, \begin{pmatrix} -0.81 \\ 44.63 \\ 2\% \end{pmatrix} \right\}$$

Downloaded 27 Jul 2011 to 140.116.71.27. Redistribution subject to ASME license or copyright; see http://www.asme.org/terms/Terms_Use.cfm

Table 5 Bounds and variations of design variables

	Design variable	UB	LB	STD
X_1	Thickness of B-pillar inner	0.5	1.5	1
X_2	Thickness of B-pillar reinforce	0.5	1.5	1
X_3	Thickness of floor side inner	0.5	1.5	1
X_4	Thickness of cross members	0.5	1.5	1
X_5	Thickness of door beam	0.5	1.5	1
X_6	Thickness of door belt reinforce	0.5	1.5	1
X_7	Thickness of roof rail	0.5	1.5	1
X_8	Yield stress of B-pillar inner	0.192	0.750	0.1
X_9	Yield stress of floor side inner	0.192	0.750	0.1

straints, and nine design variables. Table 5 shows the design variables used in this study. Among these nine variables, the first seven are dimensions related to the structural element of the vehicle. X_8 and X_9 are material properties indicating the yielding stress of structural elements with crucial influences on safety criteria. Uncertainties exist in these design variables due to manufacturing processes or from inherent material property variations. These uncertainties are modeled as Gaussian distributions with constant STDs, shown as in Table 5. The upper bounds (UB) and the lower bounds (LB) on the mean values $\boldsymbol{\mu}_{\mathbf{X}}$ are also listed

$$\min_{\boldsymbol{\mu}_{\mathbf{X}}} \{f_1(\boldsymbol{\mu}_{\mathbf{X}}), f_2(\boldsymbol{\mu}_{\mathbf{X}})\}$$

$$\text{s.t.} \Pr[g_i(\mathbf{X}) > 0] \le P_f, \ \forall \mathbf{X} \sim N(\boldsymbol{\mu}_{\mathbf{X}}, \boldsymbol{\sigma}_{\mathbf{X}}^2)$$

where

$$f_1\text{:Weight} = 1.98 + 4.9\mu_{X_1} + 6.67\mu_{X_2} + 6.98\mu_{X_3} + 4.01\mu_{X_4} + 1.78\mu_{X_5} + 2.73\mu_{X_7}$$

$$f_2\text{:Door}_{\text{velocity}} = 16.45 - 0.489\mu_{X_3}\mu_{X_7} - 0.843\mu_{X_5}\mu_{X_6}$$

$$g_1 = 1.16 - 0.3717X_2X_4 - 0.484X_3X_9$$

$$g_2 = 29.98 + 3.818X_3 - 4.2X_1X_2 + 6.63X_6X_9 - 7.7X_7X_8$$

$$g_3 = 33.86 + 2.95X_3 - 5.057X_1X_2 - 11X_2X_8 - 9.98X_7X_8 + 22X_8X_9$$

$$g_4 = 46.36 - 9.9X_2 - 12.9X_1X_8$$

$$g_5 = 0.261 - 0.0159X_1X_2 - 0.188X_1X_8 - 0.019X_2X_7 + 0.0144X_3X_5 + 0.08045X_6X_9$$

$$g_6 = 0.214 + 0.00817X_5 - 0.131X_1X_8 - 0.0704X_1X_9 + 0.03099X_2X_6 - 0.018X_2X_7 + 0.0208X_3X_8 + 0.121X_3X_9 - 0.00364X_5X_6$$

$$g_7 = 0.74 - 0.61X_2 - 0.163X_3X_8 - 0.166X_7X_9 + 0.227X_2^2$$

$$g_8 = 4.72 - 0.5X_4 - 0.19X_2X_3$$

$$g_9 = 10.58 - 0.674X_1X_2 - 1.95X_2X_8$$

The initial lateral velocity of the 950-kg moving deformable barrier in the vehicle side crash test is 56 km/h. A vehicle must meet internal and regulated side impact requirements specific to the vehicle market. In this work, the European Enhanced Vehicle-Safety Committee side impact procedure is adopted. Several dummy safety performances are used as the criteria for occupant safety under side impact including head injury criterion, abdomen load (g_1), rib deflections (upper g_2, middle g_3, and lower g_4), and viscous criteria (upper g_5, middle g_6, and lower g_7), pubic symphysis force (g_8), and the velocity of the B-pillar at the middle point (g_9).

4.2 Results and Discussion. The β-Pareto set of the bi-objective optimization problem in Eq. (24) is obtained using the proposed method with $E^s = 0.01$ and $E^p = 0.2\%$. 50 Pareto points on the deterministic Pareto set are first obtained using the constraint method. With the given E^s, this deterministic Pareto set is approximated using three linear segments with corresponding break points [24.25, 15.06], [32.94, 13.45], and [34.09, 13.45], respectively. The resulting Pareto approximation $\hat{\mathcal{P}}^0$ is listed in Table 6. Although the failure probability limit without constraint activity change is 1%, the nonlinearity in the constraints restricts the shift of the deterministic Pareto to $P_f = 14\%$.

Table 6 β-Pareto set data for Fig. 10

$$\hat{\mathcal{P}}_1^0 : \left\{ \begin{pmatrix} 23.36 \\ 15.7 \\ 1\% \end{pmatrix}, \begin{pmatrix} 25.14 \\ 14.43 \\ 1\% \end{pmatrix}, \begin{pmatrix} 27.87 \\ 14.19 \\ 1\% \end{pmatrix}, \begin{pmatrix} 32.94 \\ 13.94 \\ 1\% \end{pmatrix} \right\}$$

$$\hat{\mathcal{P}}_2^0 : \left\{ \begin{pmatrix} 23.36 \\ 16.68 \\ 1\% \end{pmatrix}, \begin{pmatrix} 25.14 \\ 14.92 \\ 1\% \end{pmatrix}, \begin{pmatrix} 27.87 \\ 14.19 \\ 1\% \end{pmatrix}, \begin{pmatrix} 32.94 \\ 13.45 \\ 1\% \end{pmatrix} \right\}$$

$$\hat{\mathcal{P}}_3^0 : \left\{ \begin{pmatrix} 23.15 \\ 16.18 \\ 1\% \end{pmatrix}, \begin{pmatrix} 24.93 \\ 14.92 \\ 1\% \end{pmatrix}, \begin{pmatrix} 27.66 \\ 14.19 \\ 1\% \end{pmatrix}, \begin{pmatrix} 32.94 \\ 13.45 \\ 1\% \end{pmatrix} \right\}$$

$$\hat{\mathcal{P}}_1^1 : \left\{ \begin{pmatrix} 24.10 \\ 15.64 \\ 1\% \end{pmatrix}, \begin{pmatrix} 25.77 \\ 14.46 \\ 1\% \end{pmatrix}, \begin{pmatrix} 28.32 \\ 14.21 \\ 1\% \end{pmatrix}, \begin{pmatrix} 33.03 \\ 13.97 \\ 1\% \end{pmatrix} \right\}$$

$$\hat{\mathcal{P}}_2^1 : \left\{ \begin{pmatrix} 24.10 \\ 15.64 \\ 1\% \end{pmatrix}, \begin{pmatrix} 25.77 \\ 14.46 \\ 1\% \end{pmatrix}, \begin{pmatrix} 28.32 \\ 14.21 \\ 1\% \end{pmatrix}, \begin{pmatrix} 33.03 \\ 13.97 \\ 1\% \end{pmatrix} \right\}$$

$$\hat{\mathcal{P}}_3^1 : \left\{ \begin{pmatrix} 24.11 \\ 15.90 \\ 1\% \end{pmatrix}, \begin{pmatrix} 25.78 \\ 14.72 \\ 1\% \end{pmatrix}, \begin{pmatrix} 28.33 \\ 14.21 \\ 1\% \end{pmatrix}, \begin{pmatrix} 33.04 \\ 13.54 \\ 1\% \end{pmatrix} \right\}$$

$$\hat{\mathcal{P}}_4^1 : \left\{ \begin{pmatrix} 23.93 \\ 16.07 \\ 1\% \end{pmatrix}, \begin{pmatrix} 25.60 \\ 14.88 \\ 1\% \end{pmatrix}, \begin{pmatrix} 28.15 \\ 14.21 \\ 1\% \end{pmatrix}, \begin{pmatrix} 33.05 \\ 13.54 \\ 1\% \end{pmatrix} \right\}$$

The proposed method needs to be repeated with Pareto points at $P_f = 14\%$ identified using the constraint method. Four new linear segments are obtained to meet the E^s requirement with break points [24.95, 15.04], [25.77, 14.46], [31.25, 13.80], and [34.09, 13.54]. The Pareto approximation $\hat{\mathcal{P}}^1$ is listed in Table 6. Within the E^p requirement, the β-Pareto set up to $P_f = 1\%$ can be obtained.

Figure 10 compares the β-Pareto set of the vehicle crashworthiness study obtained using the proposed method (solid lines) with that obtained using the constraint method ($\star$). As can be seen, the proposed method is able to capture the Pareto set with high

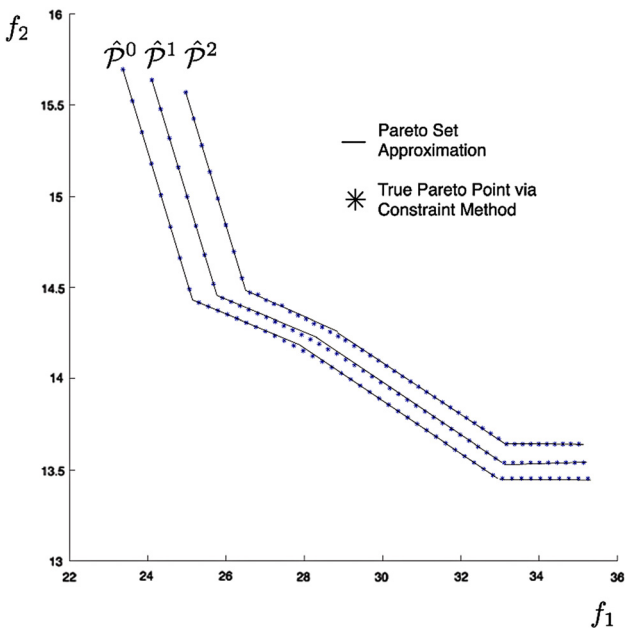

Fig. 10 β-Pareto set approximation of vehicle crashworthiness example

Downloaded 27 Jul 2011 to 140.116.71.27. Redistribution subject to ASME license or copyright; see http://www.asme.org/terms/Terms_Use.cfm

accuracy with a significant efficiency improvement. Another important feature of the proposed method is that predictions between objective trade-offs at untested P_f values can quickly be obtained without additional optimization processes. For example, if a designer would like to know the trade-off between weight and door intrusion velocity at a 95% reliability level ($P_f = 0.05$), he/she can simply use $\hat{\mathcal{P}}^1$ and $\hat{\mathcal{P}}^2$ to obtain the Pareto approximation at $P_f = 5\%$ as

$$\hat{\mathcal{P}}_{95\%} = \left\{ \begin{pmatrix} 24.50 \\ 15.61 \end{pmatrix}, \begin{pmatrix} 26.10 \\ 14.47 \end{pmatrix}, \begin{pmatrix} 28.56 \\ 14.23 \end{pmatrix}, \begin{pmatrix} 33.10 \\ 13.58 \end{pmatrix} \right\}$$

5 Concluding Remarks

Design under uncertainty is a field with growing interest that studies practical engineering problems in an analytical manner. In this work, we extend the field of design under uncertainty to multiple objectives. The main contribution of the proposed work is that we are able to predict a Pareto set at any reliability value. This allows designers to make better decisions when considering reliability. An exact β-Pareto set generation method is proposed for bi-objective linear programming problems. By identifying extreme point on the Pareto set and then calculating the vertexes, the exact Pareto set of a BOLP can be obtained. The entire β-Pareto set at all P_f values can then be constructed by calculating the Pareto set shift at various reliability levels and the limit of failure probability when constraint activity changes. We also extend the method of generating BOLP β-Pareto sets to nonlinear problems. A sandwich method is first applied to approximate the deterministic Pareto set as a union of several LP subproblems. By combing information from LP subproblems, we can construct the β-Pareto set of nonlinear problems.

The proposed method provides an efficient way for understanding the trade-offs between objectives at any reliability values. For general engineering design, this information is crucial for decision-makers for obtaining a quick and relatively accurate estimate. One needs to be aware that, when approximating a BONLP with a number of BOLPs, the resulting linear constraints might result in degeneracy. The simplex method used for obtaining the vertexes of the Pareto in Secs. 2 and 3 will not converge. Before LP problems can be solved, the standard approaches described in Ref. [18] might be necessary to ensure that redundant constraints are properly removed.

Acknowledgements

The authors would like to thank Professor Yi-Hsin Liu for illuminating certain aspects of his work in Ref. [12]. This work was partially supported by the National Science Council in Taiwan under Grant No. NSC97-2221-E-006-068.

Appendix

A.1 Activity of Probabilistic Constraints

In standard deterministic NLP, an inequality constraint is active if removing the constraint changes the optimum [19]. For simplicity of presentation, assume that a unique optimum exists and let the feasible set $\mathcal{F}$ be the union of all constraint sets $\mathcal{K}_j = \{\mathbf{x} : g_j(\mathbf{x}) \leq 0\}, j = 1, \ldots, m$. The optimum with all inequality constraints present is defined as $\mathbf{x}^* = \arg\min f(\mathbf{x}), \forall \mathbf{x} \in \mathcal{F}$, while the optimum with constraint g_j removed is defined as $\mathbf{x}_j^* = \arg\min f(\mathbf{x}), \mathbf{x} \in \mathcal{F} - \mathcal{K}_j$. From the definition of an optimum, $f(\mathbf{x}^*) \geq f(\mathbf{x}_j^*)$. Constraint g_j is active if $f(\mathbf{x}^*) \neq f(\mathbf{x}_j^*)$.

Pomrehn and Papalambros. [20] described various activity definitions for continuous constraints with continuous and discrete variables, as shown in Table 7. These definitions are adopted and extended for probabilistic constraints. The activity of a probabilistic constraint can be defined similarly: A probabilistic constraint is active if removing the constraint changes the value of the optimum. For any design vector $\boldsymbol{\mu}_\mathbf{X}$, G_j has the same feasibility information as the probabilistic constraint in

$$G_j(\boldsymbol{\mu}_\mathbf{X}) \equiv \Pr[g_j(\mathbf{X}) > 0] - P_{f,j} \tag{A1}$$

Hence, G_j is a deterministic equivalent constraint function that can be used to represent the activity of the probabilistic constraint function $\Pr[g_j(\mathbf{X}) > 0] - P_{f,j}$. Assuming G_j is a continuous differentiable function, the definitions in Table 7 can be extended simply by replacing g_j with G_j.

A.2 Relations Between $\mathcal{F}_p$ and P_f

Theorem 2. *Let $P_{f,i}$ and $P_{f,j}$ be different failure probability values in Eq. (1) and the corresponding probabilistic feasible space be $\mathcal{F}_{p,i}$ and $\mathcal{F}_{p,j}$, respectively. With an increase of reliability requirements, hence a decrease of P_f values, $\mathcal{F}_p$ shrinks as*

$$P_{f,i} \leq P_{f,j} \Rightarrow \mathcal{F}_{p,i} \subseteq \mathcal{F}_{p,j} \tag{A2}$$

Proof. Denote $\mathbf{g}'_i$ and $\mathbf{g}'_j$ as the active constraints of Eq. (1) with failure probabilities $P_{f,i}$ and $P_{f,j}$, respectively. Let the corresponding deterministic constraints set $\mathcal{K}_i = \mathcal{K}_j$. $\mathcal{F}_{p,i} \cap \mathcal{F}_{p,j} = \mathcal{F}_{p,i}$ or $\mathcal{F}_{p,j}$. Let us now prove Theorem 2 by contradiction. Assume that there exist $P_{f,i}$ and $P_{f,j}$ such that $\mathcal{F}_{p,i} \supset \mathcal{F}_{p,j}$. In optimization theory, a larger feasible space will yield a better solution than a smaller one; therefore

$$\begin{aligned} &\max\{\Pr[g_j(\mathbf{X}(\boldsymbol{\mu}_\mathbf{X})) > 0], \forall \boldsymbol{\mu}_\mathbf{X} \in \mathcal{F}_{p,i}\} \geq \\ &\quad \max\{\Pr[g_j(\mathbf{X}(\boldsymbol{\mu}_\mathbf{X})) > 0], \forall \boldsymbol{\mu}_\mathbf{X} \in \mathcal{F}_{p,j}\} \end{aligned} \tag{A3}$$

Equation (A3) also implies $P_{f,i} \geq P_{f,i}$, which contradicts our initial statement in Eq. (A2). In addition, for cases which $\mathcal{F}_{p,i} \cap \mathcal{F}_{p,j} = \emptyset$, $\mathcal{F}_{p,i} \cap \mathcal{F}_{p,j} \neq \mathcal{F}_{p,i}$, or $\mathcal{F}_{p,j}$, the initial assumptions are violated. Thus, Theorem 2 is proved. □

A.3 Linear Constraint Boundary Shift Under Random Uncertainties

Uncertainties in Eq. (5) result in probabilistic constraints, as in Eq. (4). Since we only consider $\mathbf{X}$ with Gaussian distributions, a linear constraint $g_j(\mathbf{X}) = \mathbf{A}_j^T\mathbf{X} - \mathbf{b}$ will also be Gaussian with mean μ_{gj} and variance $\sigma_{g_j}^2$, where

Table 7 Constraint activity definitions

	g_j Satisfied as a strict inequality at the optimum	g_j Satisfied as an equality at the optimum
Removal of g_j does not affect the set of optimal solutions	Inactive	Tight
Removal of g_j alters the set of optimal solutions, but does not affect its objective function value	Weakly semi-active	Strongly semi-active
Removal of g_j alters both the optimal solution set and its objective function value	Weakly active	Strongly active

Downloaded 27 Jul 2011 to 140.116.71.27. Redistribution subject to ASME license or copyright; see http://www.asme.org/terms/Terms_Use.cfm

$$\mu_{g_j} = \mathbf{A}_j^T \boldsymbol{\mu}_{\mathbf{X}} - \mathbf{b}$$
$$\sigma_{g_j}^2 = \sum_{i=1}^{n} \left(\frac{\partial g_j}{\partial x_i}\bigg|_{\boldsymbol{\mu}_{\mathbf{X}}} \right)^2 \cdot \sigma_{X_i}^2 \tag{A4}$$

The probabilistic linear constraint can then be written as the deterministic constraint g_j with a deviation Δ_j or as an equivalent deterministic constraint G_j in Eq. (A5), where

$$\begin{aligned} &\Delta_j = \sigma_{g_j} \Phi\left(1 - P_{f,j}\right) \\ &\Pr[g_j(\mathbf{X}) > 0] \le P_{\mathrm{f}} \Rightarrow \Phi\left(\mu_{g_j}/\sigma_{g_j}\right) - P_{\mathrm{f}} \le 0 \\ &\Rightarrow g_j(\mu_{\mathbf{X}}) + \Delta_j \le 0 \equiv G_j(\boldsymbol{\mu}_{\mathbf{X}}) \le 0 \end{aligned} \tag{A5}$$

Theorem 3. *Constraint deviations* $\boldsymbol{\Delta}$ *in Eq. (A5) due to* P_f *result in a constant shift to the Pareto set* $\mathcal{P}$ *if constraint activity remains unchanged.*

Proof. Let us now compare the Pareto frontiers along the active constraints $\mathbf{g}$ and the probabilistic active constraint $\mathbf{g}'$ of the same active set $\mathcal{G}$. The vertex of the active set $\mathcal{G}$ is the solution of the simultaneous equations, as shown

$$\mathbf{x}_k^* = \{\mathbf{g} : \mathbf{A}^T\mathbf{x} - \mathbf{b} = 0,\ \mathbf{g} \in \mathcal{G}\} \tag{A6}$$

Assuming that the active set remains unchanged, the vertex of the β-Pareto is $\mathbf{x}_k'^*$ such that

$$\mathbf{x}_k'^* = \{\mathbf{g}' : \mathbf{A}^T\mathbf{x} - \mathbf{b} + \Delta = 0,\ \mathbf{g}' \in \mathcal{G}\} \tag{A7}$$

The shift of constraint boundaries results in the vector

$$\mathbf{d}_x = \mathbf{x}_k - \mathbf{x}'_k = \mathbf{A}^{-1}\Delta \tag{A8}$$

If we calculate the effect of the constraint shift on the objective space, we have

$$\mathbf{d}_f = \mathbf{f}' - \mathbf{f} = \mathbf{C}^T\mathbf{A}^{-1}\Delta \tag{A9}$$

Theorem 4. *Without changing constraint activity, the shift of* $\mathcal{P}$ *is proportional to* $\left(-\Phi^{-1}(1 - P_{\mathrm{f}})\right)$.

Proof. $\boldsymbol{\Delta}$ in Eq. (A9) is proportional to $\left(-\Phi^{-1}(1 - P_{\mathrm{f}})\right)$ based on Eq. (A5). The shift of Pareto $\mathbf{d}_f$ in Eq. (A9) is therefore proportional to $\left(-\Phi^{-1}(1 - P_{\mathrm{f}})\right)$.

Nomenclature

$\mathcal{A}$ = attainable set, with $\hat{\mathcal{A}}$ being its approximation
E^s = error in Pareto set approximation obtained using the sandwich method
E^p = error in β-Pareto approximation of nonlinear problems
$\mathcal{F}$ = feasible space with deterministic constraints $\mathbf{g} \le 0$
$\mathcal{F}_p(P_{\mathrm{f}})$ = feasible space with probabilistic constraints $\Pr[g_j > 0] \le P_{\mathrm{f}}, \forall j \in \mathcal{K}$
$\mathbf{f}(\mathbf{x})$ = objective functions to be optimized with respect to $\mathbf{x}$
$\mathbf{f}_i^*$ = extreme point on the Pareto set with respect to the ith objective
$\mathbf{f}^*$ = a point on the Pareto set, with $\hat{\mathbf{f}}^*$ being its approximation
$\bar{\mathbf{f}}$ = vertex of the Pareto frontier
$\mathbf{f}'$ = breakpoint of a Pareto approximation
g_j = the jth deterministic constraint in the negative null form, $j = 1, \ldots, m$
G_j = equivalent deterministic constraint of $\Pr[g_j > 0] - P_{\mathrm{f}}$
$\mathcal{K}$ = constraint set
n = number of design variables (problem dimensions)
$\mathcal{P}$ = deterministic Pareto set, with $\hat{\mathcal{P}}$ being its approximation
$\mathcal{P}_\beta$ = β-Pareto set
$\mathbf{Pr}[\cdot]$ = probability of $\cdot$
P_{f} = failure probability levels
P'_{f} = limit of failure probability without change of constraint activity
$\mathbf{R}$ = reduced cost coefficient
$\mathbf{S}$ = frame of $\mathbf{R}$
$\mathbf{x}$ = deterministic design variables
X = Gaussian random variable with mean μ_X and standard deviation σ_X
Z = standard Gaussian random variable with zero mean and unity variance
β = reliability index
(N)LP = (non)linear programming
BO(N)LP = bi-objective (non)linear programming
RBDO = reliability-based design optimization

References

[1] Li, Z., Izquierdo, L., Kokkolaras, M., Hu, J., and Papalambros, P., 2008, "Multiobjective Optimization for Integrated Tolerance Allocation and Fixture Layout Design in Multistation Assembly," ASME J. Manuf. Sci. Eng., **130**, p. 044501.
[2] Li, Z., Kokkolaras, M., Papalambros, P., and Hu, J., 2005, "An Optimization Study of Manufacturing Variation Effects on Diesel Injector Design With Emphasis on Emissions," SAE Paper, 2004–01–1560.
[3] Levi, F., Gobbi, M., and Mastinu, G., 2005, "An Application of Multi-Objective Stochastic Optimisation to Structural Design," Struct. Multidiscip. Optim., **29**(4), pp. 272–284.
[4] Singh, A., and Minsker, B., 2008, "Uncertainty-Based Multiobjective Optimization of Groundwater Remediation Design," Water Resour. Res., **44**(2), pp. 1–20.
[5] Caballero, R., Cerda, E., Munoz, M., Rey, L., and Stancu-Minasian, I., 2001, "Efficient Solution Concepts and Their Relations in Stochastic Multiobjective Programming," J. Optim. Theory Appl., **110**(1), pp. 53–74.
[6] Caballero, R., Cerda, E., Munoz, M., and Rey, L., 2004, "Stochastic Approach Versus Multiobjective Approach for Obtaining Efficient Solutions in Stochastic Multiobjective Programming Problems," Eur. J. Oper. Res., **158**(3), pp. 633–648.
[7] Ben-Abdelaziz, F., Lang, P., and Nadeau, R., 1995, "Distributional Efficiency in Multiobjective Stochastic Linear Programming," Eur. J. Oper. Res., **85**, pp. 399–415.
[8] Rommelfanger, H., 2007, "A General Concept for Solving Linear Multicriteria Programming Problems With Crisp, Fuzzy or Stochastic Values," Fuzzy Sets Syst., **158**(14), pp. 1892–1904.
[9] Tonon, F., Mammino, A., and Bernardini, A., 2002, "Multiobjective Optimization Under Uncertainty in Tunneling: Application to the Design of Tunnel Support/Reinforcement With Case Histories," Tunnelling Underground Space Technol., **17**, pp. 33–54.
[10] Gass, S., and Saaty, T., 1955, "The Computational Algorithm for the Parametric Objective Function," Nav. Res. Logistics Quart., **2**, p. 39.
[11] Marglin, S., 1967, *Public Investment Criteria*, MIT, Cambridge, MA.
[12] Dauer, J., and Liu, Y., 1990, "Solving Multiple Objective Linear Programs in Objective Space," Eur. J. Oper. Res., **46**(3), pp. 350–357.
[13] Wets, R., and Witzgall, C., 1967, "Algorithms for Frames and Lineality Spaces of Cones," J. Res. Natl. Bur. Stand., **71B**(1), pp. 1–7.
[14] Chan, K.-Y., Skerlos, S., and Papalambros, P., 2007, "An Adaptive Sequential Linear Programming Algorithm for Optimal Design Problems With Probabilistic Constraints," ASME J. Mech. Des., **29**(2), pp. 140–149.
[15] Yang, X., and Goh, C., 1997, "A Method for Convex Curve Approximation," Eur. J. Oper. Res., **97**, pp. 205–212.
[16] Gu, L., Yang, R.-J., Tho, C., Makowski, M., Faruque, O., and Li, Y., 2001, "Optimization and Robustness for Crashworthiness of Side Impact," Int. J. Veh. Des., **26**(4), pp. 348–360.
[17] Sinha, K., 2007, "Reliability-Based Multiobjective Optimization for Automotive Crashworthiness and Occupant Safety," Struct. Multidiscip. Optim., **33**(3), pp. 255–268.
[18] Fletcher, R., 1987, *Practical Methods of Optimization*, 2nd ed., John Wiley & Sons, New York.
[19] Papalambros, P., and Wilde, D., 2000, *Principles of Optimal Design*, 2nd ed., Cambridge University Press, New York.
[20] Pomrehn, L., and Papalambros, P., 1994, "Global and Discrete Constraint Activity," ASME J. Mech. Des., **116**(3), pp. 745–748.

Downloaded 27 Jul 2011 to 140.116.71.27. Redistribution subject to ASME license or copyright; see http://www.asme.org/terms/Terms_Use.cfm